Eur. Phys. J. D **31**, 189–194 (2004)
DOI: 10.1140/epjd/e2004-00136-9

THE EUROPEAN PHYSICAL JOURNAL D

Photoassociative formation of ultracold polar KRb molecules

S. Kotochigova[a], E. Tiesinga, and P.S. Julienne

National Institute of Standards and Technology, 100 Bureau Drive, stop 8423, Gaithersburg, Maryland 20899, USA

Received 11 June 2004
Published online 19 October 2004 –

Abstract. We investigate the effectiveness of creating polar ground-state KRb molecules by two-color photoassociative spectroscopy. In this process the molecules are formed from ultra-cold samples of K and Rb. Focusing on spin-polarized atoms we show that an effective pathway exists. In addition, we investigate the stability of the polar molecules in the presence of a thermal black-body radiation field.

PACS. 32.80.Pj Optical cooling of atoms; trapping – 34.20.Cf Interatomic potentials and forces – 33.70.Ca Oscillator and band strengths, lifetimes, transition moments, and Franck-Condon factors – 34.50.-s Scattering of atoms and molecules

1 Introduction

Photoassociative formation of ultracold molecules was first proposed by Thorsheim et al. [1]. A schematic picture of this process is shown in Figure 1. Two colliding ground state atoms absorb a photon to create an excited molecule. This state can decay by spontaneous emission to various vibrational levels of the ground-state molecule. The molecules are expected to have a temperature comparable to that of the atoms from which they have formed. Several years later Band and Julienne [2] modified the initial proposal by introducing a second laser, which makes ground-state molecules by stimulated emission. Quantitative modeling of two-photon photoassociative production of molecules has been developed in reference [3].

Cold ground-state alkali-metal molecules have been created by optical means in Magneto-Optical Traps starting from atoms at temperatures on the order of 100 μK and in Bose condensates with atoms on the order of and below a nK [4]. These homonuclear molecules are produced in high-lying vibrational states close to the atomic dissociation limit.

In a theoretical proposal Jaksch et al. [5] suggest a photoassociative mechanism to produce ultracold Rb_2 molecules in the lowest vibrational levels of its ground state $X^1\Sigma_g^+$ potential. They have shown that 6 to 7 transitions are needed to form the homonuclear molecule in the $v = 0$ vibrational level. Rate limiting Franck-Condon factors prevent a direct two-photon production of molecules in low v vibrational levels. The ground- and excited-state potentials used in photoassociation have very different dependence on internuclear separation R, which greatly limits the range of vibrational states with favorable transition matrix elements.

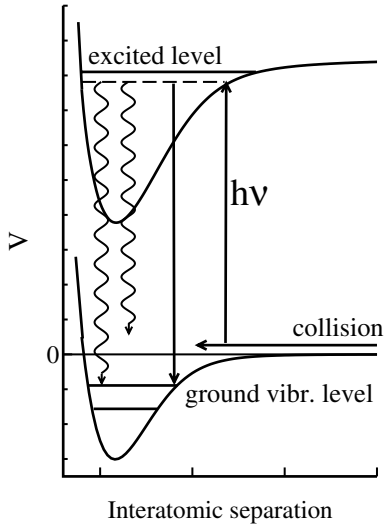

Fig. 1. A schematic diagram of the formation of ultra-cold molecules from two colliding atoms. Full horizontal lines represent molecular levels. Vertical lines with arrows indicate the stimulated absorption or emission of a photon. Sinusoidal lines indicate spontaneous emission from excited molecular levels.

On the other hand, as discussed by Wang and Stwalley [6], there is hope that the number of transitions might be reduced for heteronuclear alkali-metal systems. In heteronuclear molecules Franck-Condon factors can be more favorable in the photoassociation process. The long-range potential shape of both ground and excited states is given by an induced-dipole induced-dipole C_6/R^6 potential. Among the different heteronuclear alkali-metal diatomic molecules K+Rb and Rb+Cs have an exceptionally large C_6 dispersion coefficient for the excited states, and, consequently, a better match between ground and

[a] e-mail: svetlana@nist.gov

excited curves. Recently experimental groups from the University of Connecticut and Yale University in collaboration with Bergeman have started to investigate the possibility for photoassociative production of KRb [7] and RbCs [8] molecules, respectively.

In a previous paper [9] we made the first steps towards obtaining practical guidelines for photoassociatively producing low v vibrational states of the heteronuclear KRb molecules. We calculated the electronic transition dipole moments between ground state K and Rb and excited state potentials. In addition, we obtained the permanent dipole moments of the polar $X^1\Sigma^+$ and $a^3\Sigma^+$ ground states. A relativistic electronic structure code was used.

We also discussed the possibility of creating $X^1\Sigma^+$ molecules starting from doubly spin-polarized K and Rb atoms via two-photon photoassociation. These atoms collide on the triplet $a^3\Sigma^+$ potential, which makes the production of molecules in the X state problematic, since a direct transition between the triplet and singlet spin manifold is forbidden. We found, however, that for photon energies close to the transition energy between the ^2S and ^2P_j states of Rb a pathway exists. Excited molecular vibrational levels are then described by the Hund's case (c) coupling scheme and the projection Ω of the electronic total angular momentum on the molecular axis is an approximately good quantum number. Excited $\Omega = 0$ or 1 states have both singlet and triplet character, and stimulated transitions from the triplet state to excited Ω states followed by a downward transition to the ground singlet state exist. This process is absent in homonuclear dimers, since the additional gerade-ungerade symmetry prevents it.

In this paper we further study the production of ultracold KRb molecules in order to determine, which ground and excited vibrational states are optimal for two-photon Raman photoassociation. We do this by calculating Franck-Condon factors between rovibrational levels of the singlet-$X^1\Sigma^+$ and triplet-$a^3\Sigma^+$ on the one hand and vibrational levels of the excited Ω potentials on the other.

We also determine the lifetime of the $X^1\Sigma^+$ and $a^3\Sigma^+$ vibrational levels in the presence of thermal black-body radiation. If all population is initially put into a single rovibrational state by a laser-induced Raman transition, this coupling between molecule and thermal radiation can rapidly diffuse the population to nearby states. In general, this effect might be significant, as the energy spacing between rovibrational levels can be on the order of k_BT at room temperature, where k_B is the Boltzman constant.

We first describe the coupling to black-body radiation and then discuss molecule production.

2 Black body radiation

The role of black-body radiation in redistributing population among rovibrational levels of the singlet $X^1\Sigma^+$ and triplet $a^3\Sigma^+$ states can be estimated from the permanent dipole moments, $d(R)$, obtained in reference [9]. From reference [9] we find that at the equilibrium separation of the singlet and triplet states the electronic dipole moments are $-0.30(2)\ ea_0$ and $-0.02(1)\ ea_0$, respectively. Here, e is the electron charge, 1 $a_0 = 0.0529$ nm is the Bohr radius, and the numbers in parenthesis are one-standard-deviation uncertainties.

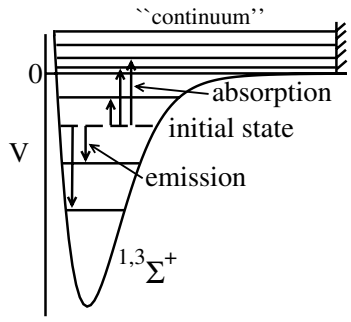

Fig. 2. A schematic diagram of the absorption and (spontaneous and stimulated) emission of a photon starting from an initial rovibrational level vlm. The final state can have different rotational angular momentum l' or l''. The figure also shows the discretization of the continuum of two free colliding atoms.

Each rovibrational level of the singlet and triplet state is labeled by vlm, where v is the vibrational quantum number, l is the nuclear orbital angular momentum, and m the projection of l along a space-fixed axis. For the purposes of this paper fine- and hyperfine-coupling is neglected. Consequently, the lifetime of singlet and triplet levels can be treated separately. The energy of a rovibrational level is denoted by E_{vl} and independent of m.

Photons of the black-body radiation can be absorbed or emitted by a molecular level. A schematic diagram of the processes is shown in Figure 2. The total transition rate from a rovibrational state can be written as

$$\Gamma^{tot}_{vlm} = \Gamma^{BB}_{vlm} + \Gamma^{spont}_{vlm}; \tag{1}$$

the sum of a black-body (BB) and a spontaneous-emission contribution. In fact,

$$\Gamma^{BB}_{vlm} = \sum_{v'l'm'} \bar{n}(\omega_{v'l'}) \Gamma^{emis}(vlm \to v'l'm') + \sum_{v''l''m''} \bar{n}(\omega_{v''l''}) \Gamma^{abs}(vlm \to v''l''m'') \tag{2}$$

and

$$\Gamma^{spont}_{vlm} = \sum_{v',l'm'} \Gamma^{emis}(vlm \to v'l'm'), \tag{3}$$

where the indices $v'l'm'$ and $v''l''m''$ denote rovibrational levels with an energy that is smaller and larger than that of vlm, respectively. Equation (3) and the first term of equation (2) describe the emission of a photon; the second term of equation (2) describes the absorption. The sum over $v''l''m''$ includes the contribution of the continuum of two free atoms as a photon can break the bond of a dimer. The factor $\bar{n}$ corresponds to the average number of photons in an electromagnetic mode at frequency ω and is given by

$$\bar{n}(\omega) = \frac{1}{e^{-\hbar\omega/k_BT} - 1},$$

where $\hbar$ is Planck's constant. Finally, $\hbar\omega_{v'l'}$ denotes the energy difference between $E_{v'l'}$ and E_{vl} and $\hbar\omega_{v''l''}$ denotes the energy difference between $E_{v''l''}$ and E_{vl}.

The emission, Γ^{emis}, and absorption, Γ^{abs}, rates that describe the individual contributions are proportional to the square of the vibrationally averaged dipole moment and are given by

$$\Gamma^{\alpha}(vlm \to v'l'm') = \frac{8\pi}{3}\frac{1}{hc^3}\omega^3|\langle|d|\rangle|^2 \qquad (4)$$

where α is either *emis* or *abs*, $\hbar\omega$ is the energy difference of the two rovibrational states vlm and $v'l'm'$, and the vibrationally-averaged dipole moment $\langle|d|\rangle = \langle v'l'm'|d(R)Y_{1q}(\hat{R})|vlm\rangle$ with $d(R)$ the R-dependent dipole moment of either the singlet or triplet potential, Y_{1q} a spherical harmonic, $\hat{R}$ the orientation of the molecule in the space-fixed coordinate system, and $q = m - m'$. The selection rules of the vibrationally-averaged dipole moment ensure $|l - l'| \leq 1$ and $|m - m'| \leq 1$.

The rovibrational wavefunctions $|vl\rangle$ and energies are obtained for the potential $V_{x,a}(R) + \hbar^2 l^2/(2\mu R^2)$, where $V_{x,a}(R)$ is either the $X^1\Sigma^+$ or $a^3\Sigma^+$ potential and μ is the reduced molecular mass. We use the short-range part of the ab initio potentials obtained in reference [9] and have connected them to the most accurate determination of the long-range dispersion and exchange potential [10]. The short-range ab initio potential is slightly shifted in energy in order to construct a potential that agrees with known scattering length determinations [11].

We perform the nuclear-dynamics calculations using a discrete variable representation (DVR) for the Schrödinger equation [12]. The vibrationally-averaged dipole moment is then given by the overlap between the wavefunctions and the R-dependent permanent dipole moment. For the discretization a hard wall is placed at large internuclear separation. This discretizes the continuum of two free colliding atoms as indicated in Figure 2. For the transition rates the contribution of the bound and continuum states can then be treated on the same footing. We have checked that moving the hard wall to larger R and increasing the number of discretization points does not change our results.

Figure 3 shows the partial lifetimes $1/\Gamma^{BB}_{vlm}$ and $1/\Gamma^{spont}_{vlm}$ of the $X^1\Sigma^+$ $l = 0$ vibrational states as a function of their binding energy. For a radiation field at $T = 100$ K the spontaneous and black-body lifetimes are about equal, while for $T = 300$ K the black-body process limits the lifetime. The graph also shows that the lowest and highest vibrational levels live longer for both spontaneous and black-body processes. At room temperature the shortest lifetimes (200 s) occur for vibrational levels between $v = 70$ and 80 and binding energies between $E/h = -100\,\mathrm{cm}^{-1}$ and $-1000\,\mathrm{cm}^{-1}$. This lifetime is much longer than the typical duration of ultra-cold experiments. In a recent paper Zemke and Stwalley [13] calculated the spontaneous emission lifetime of rovibrational levels of the $X^1\Sigma^+$ ground state and came to a similar conclusion for $1/\Gamma^{spont}_{vlm}$. Details of their calculation are different.

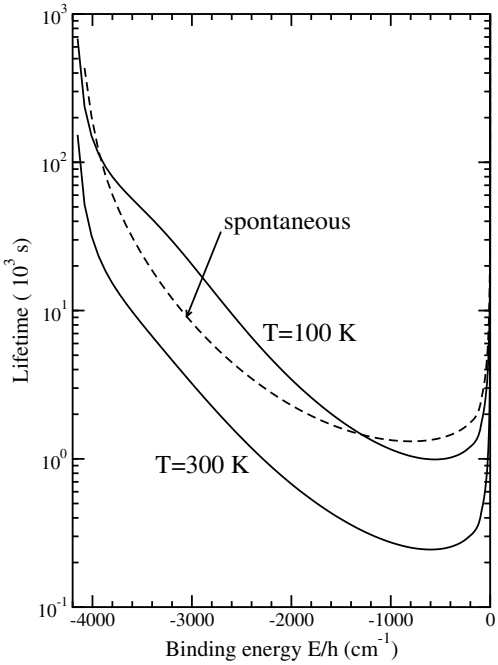

Fig. 3. The black-body and spontaneous-emission lifetime of $X^1\Sigma^+$ $l = 0$ vibrational states as a function of their binding energy. The black-body lifetime is shown for two temperatures.

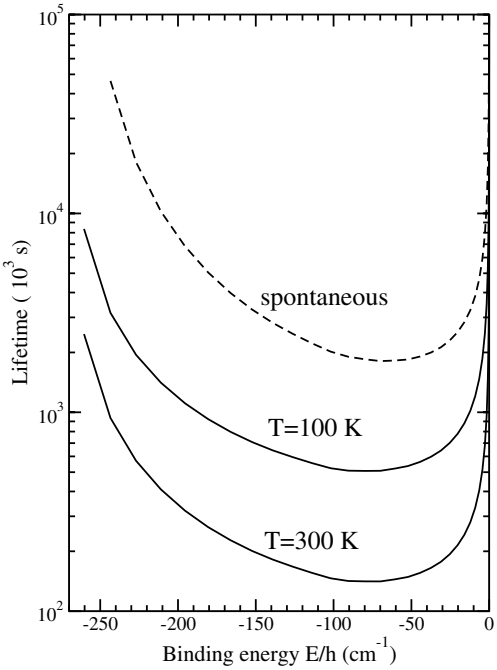

Fig. 4. The black-body and spontaneous-emission lifetime of $a^3\Sigma^+$ $l = 0$ vibrational states as a function of their binding energy. The black-body lifetime is shown for two temperatures.

The lifetime of the $X^1\Sigma^+$ $l = 1$ rotational levels is of the same order of magnitude as those of $l = 0$. The blackbody and spontaneous-emission lifetime of the $a\,^3\Sigma^+$ $l = 0$ vibrational levels is shown in Figure 4. It is on the order of 10^5 s to 10^6 s and significantly longer than that of the X state.

The long lifetime and, therefore, the small rate is predominantly due to the interplay between the ω^3 and $|\langle d\rangle|^2$ terms in equation (4) as a function of the frequency difference between the initial vl and final $v'l'$ or $v''l''$ states. Vibrational transitions with $\Delta v = v' - v \neq 0$ have energy differences that are orders of magnitude larger than the energy differences of rotational transitions with $\Delta v = 0$ and $\Delta l = l' - l \neq 0$. Consequently, the ω^3 term favors vibrational transitions. For the $X^1\Sigma^+$ potential of K+Rb the energy difference of the $v = 0 \rightarrow v'' = 1$ vibrational transition is $\sim$100 cm^{-1}, while the energy difference of the $v = 0, l = 0 \rightarrow v'' = 0, l'' = 1$ rotational transition is $\sim$0.1 cm^{-1}. Both vibrational $|\Delta v| = 1$ and rotational $|\Delta l| = 1$ spacings decrease with v.

The square of the vibrational averaged dipole moment $|\langle d\rangle|^2$ has a rather different frequency dependence. This quantity is orders of magnitude larger for rotational transitions than for vibrational transitions, which can be understood from the overlap of vibrational wavefunctions and the R dependence of the electronic dipole moment $d(R)$. Rovibrational wavefunctions with different v are orthogonal if they have the same l and nearly orthogonal when they have different l, as the rotational Hamiltonian is a small correction to the potentials. Consequently, for rotational transitions the averaged dipole moment is approximately equal to the electronic dipole moment near the outer turning point of the vibrational motion. For vibrational transitions the matrix elements are proportional to the slope of the electronic dipole moment near the outer turning point. A Taylor expansion of $d(R)$ around the outer turning point and the orthogonality of vibrational wavefunctions indicates that the actual value at the turning point is not important.

For the $X^1\Sigma^+$ and a $^3\Sigma^+$ state of KRb the vibrational transitions contribute most to the transition rates. In other words, the ω^3 dependence wins from the $|\langle d\rangle|^2$ dependence. In addition, the transition rates are proportional to the slope of the dipole moment. The slope is smallest for turning points near the $v = 0$ level, increases for vibrational levels with binding energies larger than 1000 cm^{-1}, and then decreases again. (See Figs. 2 or 3 of Ref. [9].) The inverse of this dependence is observed in the lifetimes shown in Figures 3 and 4.

3 Transition dipole moments

This section describes Franck-Condon factors for the production of ground state $^1\Sigma^+$ or $^3\Sigma^+$ rovibrational molecules via two-color Raman photoassociation starting from a pair of colliding spin-polarized K and Rb atoms. The atoms scatter on the $a^3\Sigma^+$ potential. The intermediate excited state that is of interest has 0^+ symmetry and two such relativistic excited potentials are shown in Figure 5a. The potentials were obtained from reference [9]. The two attractive potentials dissociate to the K($4s$)+Rb($5p$) atomic limit. At short internuclear separations the potentials can be approximately described by the Hund's case (a) $n^{2S+1}\Lambda^{\pm}$ symmetry, where Λ is the projection of the electron orbital angular momentum along the internuclear axis. At longer R the curves can only be described with Hund's case (c) $m(\Omega^{\pm})$ labeling and relativistic effects are important. The numbers n and m show the energy-ordered appearance of these states.

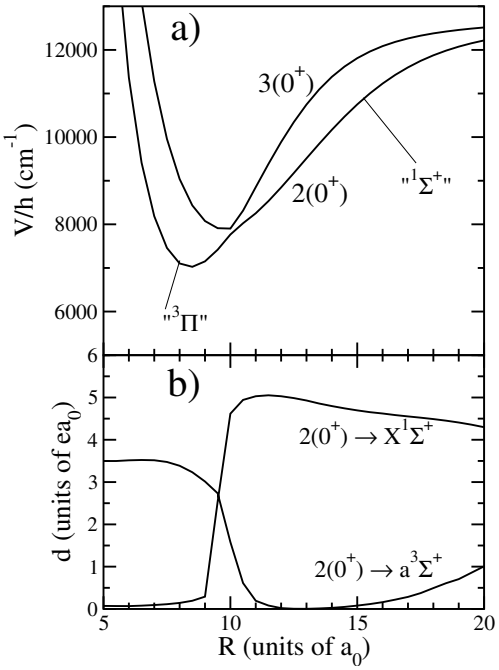

Fig. 5. Excited 0^+ electronic potentials and electronic transition dipole moments to the $X^1\Sigma^+$ and $a^3\Sigma^+$ ground states as a function of internuclear separation. Panel (a) shows the potentials and panel (b) shows the transition dipole moments.

Figure 5b shows the non-zero transition dipole moment between the $a^3\Sigma^+$ and $2(0^+)$ states and between the $X^1\Sigma^+$ and $2(0^+)$ states. We estimate that the uncertainty of the transition dipole moments is 0.1 ea_0 based on a comparison of the dipole moments at $R = 100\,a_0$ (not shown) and the known $5s$ to $5p$ dipole moment of Rb. The rapid change in dipole moment near $R = 10\ a_0$ is due to the avoided crossing between the $2(0^+)$ and $3(0^+)$ potentials seen in panel (a) of Figure 5. We verified that the $2(0^+)$ state has Hund's case (a) $^3\Pi$ character for $R < 10\ a_0$ and $^1\Sigma$ character for $R > 10\ a_0$. For $R > 15\ a_0$ the potentials can not be described with Hund's case (a) symmetry. The transition dipole moments in Figure 5b reflect this change in character. For $R < 10\ a_0$ the transition dipole moment is large to the triplet ground state as triplet to triplet transitions are allowed. Similarly, for $10\ a_0 < R < 15\ a_0$ only the transition to the singlet ground state is allowed. For $R > 15\ a_0$ both transitions are allowed.

The R dependence of the dipole moments has a strong impact on the Franck-Condon factor defined as the vibrationally averaged matrix element $O_{v'v} = |\langle 2(0^+)\, v'|d(R)|g\, v\rangle|^2$, where g is either the $X\,^1\Sigma^+$ or $a^3\Sigma^+$ state and $d(R)$ is the electronic dipole moment shown in Figure 5. For this calculation the rotational Hamiltonian and the angular dependence of the dipole moment have been neglected, as our main purpose is to show trends.

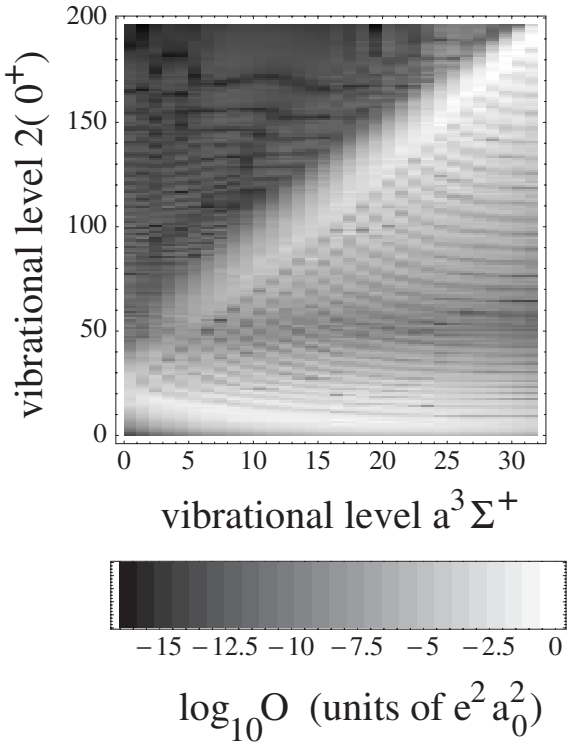

Fig. 6. The 10 logarithm of the square of the vibrationally averaged dipole moment for the transition between the $a^3\Sigma^+$ and $2(0^+)$ potential.

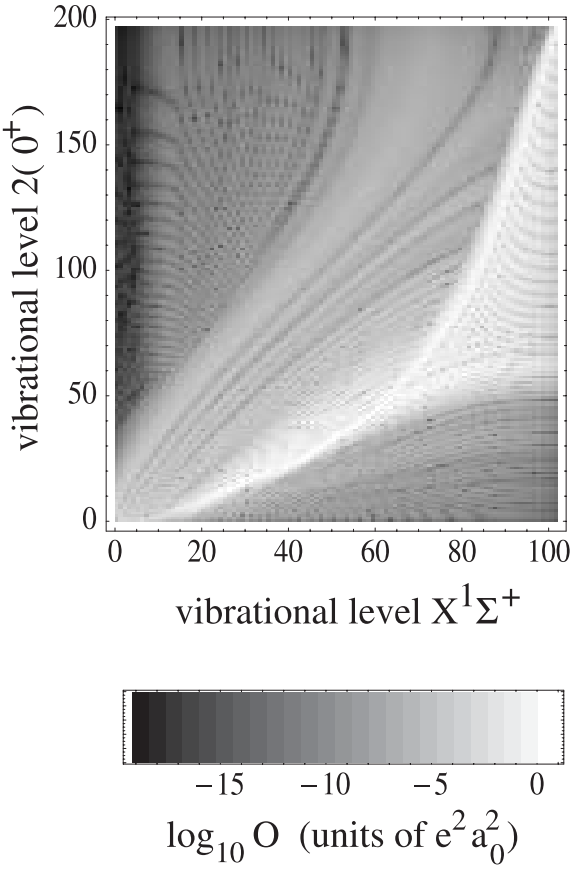

Fig. 7. The 10 logarithm of the square of the vibrationally averaged dipole moment for the transition between the $X^1\Sigma^+$ and $2(0^+)$ potential.

Figure 6 shows the density plot of $\log_{10} O_{v'v}$ for the $a^3\Sigma^+$ to $2(0^+)$ transition. The value of O is described by the gray scale. The largest values (white areas) lie between 0.01 $e^2a_0^2$ and 0.1 $e^2a_0^2$ and occur along two branches: for low ($v' \leq 10$) of the $2(0^+)$ state and along the diagonal of the figure. The former branch is nearly independent of the vibrational level of the a state.

For two-color Raman photoassociation we imagine an experiment with two trapped spin-polarized atoms, interacting via the $a^3\Sigma^+$ potential. Figure 6 only shows the vibrationally averaged dipole moment of the bound states of the a state. Nevertheless, we can make statements about the transition dipole for two scattering atoms. In our numerical calculations we discretize the continuum by placing a hard wall at large internuclear separation. The first states of this discretized continuum can be interpreted as levels of the external trap. We find that the ratio of $O_{v'v}$ of the last bound state and the first continuum state of the $a^3\Sigma^+$ potential is almost independent of the $2(0^+)$ vibrational level v'. The values of O for a continuum state, however, are several orders of magnitude smaller than that for the last bound state. The precise value depends on the actual size of the trap in an experiment. (The scale factor is proportional to the ratio of the square root of the volume of the last bound and trap state.) We conclude that matrix elements for the $a^3\Sigma^+$ continuum are largest for $v' < 10$ and $v' > 160$.

In Figure 7 Franck-Condon factors for the transition between the $X^1\Sigma^+$ and $2(0^+)$ state are shown. The pattern is rather different then that in Figure 6. The largest Franck-Condon factors are approximately ten times bigger, and shown as the white band in the graph. If we assume that we populate the lowest v' states of the $2(0^+)$ potential, starting from the $a^3\Sigma^+$ continuum, then we can reach the vibrational levels $v < 30$ of the X state. This indicates that we only need one Raman transition to produce very-deeply bound ground state KRb molecules.

The two density plots in Figures 6 and 7 can only be seen as a qualitative guide towards finding the optimal paths for the production of cold ground-state heteronuclear molecules. In the future, we wish to include the effects of mixing between the $2(0^+)$ and $3(0^+)$ states via nonadiabatic coupling. For quantitative predictions the rotation of the atoms needs to be included as well. Moreover, we want to study pathways via $\Omega = 1$ excited state potentials.

4 Conclusion

We have used published electronic potentials and dipole moments of KRb to evaluate Frank-Condon factors between vibrational levels of ground and excited state potentials and have found that there is a viable two-photon Raman transition to form low-vibrational ground-state KRb molecules. In addition, we investigated the effect of

black-body radiation on the polar molecule and find that the shortest lifetime is around 200 s, which is significantly longer than the duration of typical ultra-cold-atom experiments.

In our previous publication [9] we reported a 7% uncertainty for the permanent dipole moment of $X^1\Sigma^+$ and a 50% uncertainty for the permanent dipole moment of a $^3\Sigma^+$ state. This gives about 14% uncertainty in the lifetime of singlet state and factor of 2 uncertainty in the lifetime of triplet state. These uncertainties do not change our conclusion on the stability of KRb polar molecules to thermal radiation.

Transition dipole moments between rovibrational states of the ground and excited configurations depend on electronic dipole moments with an estimated uncertainty of about 3% [9]. This leads to an uncertainty in the rovibrational transition probabilities of about 6%. This uncertainty is insignificant for the purpose of the paper of showing trends in Franck-Condon factors.

References

1. H.R. Thorsheim, J. Weiner, P.S. Julienne, Phys. Rev. Lett. **58**, 2820 (1987)
2. Y.B. Band, P.S. Julienne, Phys. Rev. A **51**, R4317 (1995)
3. J.L. Bohn, P.S. Julienne, Phys. Rev. A **60**, 414 (1999)
4. C.C. Tsai, R.S. Freeland, J.M. Vogels, H.M.J.M. Boesten, B.J. Verhaar, D.J. Heinzen, Phys. Rev. Lett. **79**, 1245 (1997); A. Fioretti, D. Comparat, A. Crubellier, O. Dulieu, F. Masnou-Seeuws, P. Pillet, Phys. Rev. Lett. **80**, 4402 (1998); A.N. Nikolov, E.E. Eyler, X.T. Wang, J. Li, H. Wang, W.C. Stwalley, P.L. Gould, Phys. Rev. Lett. **82**, 703 (1999); F.K. Fatemi, K.M. Jones, P.D. Lett, E. Tiesinga, Phys. Rev. A **66**, 053401 (2002)
5. D. Jaksch, V. Venturi, J.I. Cirac, C.J. Williams, P. Zoller, Phys. Rev. Lett. **89**, 040402 (2002)
6. H. Wang, W.C. Stwalley, J. Chem. Phys. **108**, 5767 (1998)
7. D. Wang, J. Qi, M.F. Stone, O. Nikolayeva, B. Hattaway, S.D. Gensemer, H. Wang, T. Zemke, P.L. Gould, E.E. Eyler, W.C. Stwalley, Eur. Phys. J. D **31**, 165 (2004)
8. A.J. Kerman, J.M. Sage, S. Sainis, T. Bergeman, D. DeMille, Phys. Rev. Lett. **92**, 153001 (2004)
9. S. Kotochigova, P.S. Julienne, E. Tiesinga, Phys. Rev. A **68**, 022501 (2003)
10. A. Derevianko, J.F. Babb, A. Dalgarno, Phys. Rev. A **63**, 052704 (2001); M. Marinescu, H.R. Sadeghpour, Phys. Rev. A **59**, 390 (1999); B.M. Smirnov, M.I. Chibisov, Sov. Phys. JETP **21**, 624 (1965)
11. G. Ferrari, M. Inguscio, W. Jastrzebski, G. Modugno, G. Roati, A. Simoni, Phys. Rev. Lett. **89**, 053202 (2002); A. Simoni, F. Ferlaino, G. Roati, G. Modugno, M. Inguscio, Phys. Rev. Lett. **90**, 163202 (2003)
12. R. Meyer, J. Chem. Phys. **52**, 2053 (1970); D.T. Colbert, W.H. Miller, J. Chem. Phys. **96**, 1982 (1992); O. Dulieu, P.S. Julienne, J. Chem. Phys. **103**, 60 (1995)
13. W.T. Zemke, W.C. Stwalley, J. Chem. Phys. **120**, 88 (2004)